Published in final edited form as:
J Chromatogr A. 2010 September 3; 1217(36): 5700–5709. doi:10.1016/j.chroma.2010.07.009.

The Impact of Sampling Time on Peak Capacity and Analysis Speed in On-line Comprehensive Two-Dimensional Liquid Chromatography

Lawrence W. Potts[*],
Department of Chemistry, Gustavus Adolphus College, 800 West College Avenue, Saint Peter, MN USA 56082

Dwight R. Stoll,
Department of Chemistry, Gustavus Adolphus College, 800 West College Avenue, Saint Peter, MN USA 56082

Xiaoping Li, and
Department of Chemistry, University of Minnesota, 207 Pleasant St., S.E., Minneapolis, MN USA 55455

Peter W. Carr
Department of Chemistry, University of Minnesota, 207 Pleasant St., S.E., Minneapolis, MN USA 55455

Abstract

Comprehensive two-dimensional liquid chromatography (2DLC) offers a number of practical advantages over optimized one-dimensional LC in peak capacity and thus in resolving power. The traditional “product rule” for overall peak capacity for a 2DLC system significantly overestimates peak capacity because it neglects under-sampling of the first dimension separation. Here we expand on previous work by more closely examining the effects of the first dimension peak capacity and gradient time, and the second dimension cycle times on the overall peak capacity of the 2DLC system. We also examine the effects of re-equilibration time on under-sampling as measured by the under-sampling factor and the influence of molecular type (peptide vs. small molecule) on peak capacity. We show that in fast 2D separations (less than one hour), the second dimension is more important than the first dimension in determining overall peak capacity and conclude that extreme measures to enhance the first dimension peak capacity are usually unwarranted. We also examine the influence of sample types (small molecules vs. peptides) on second dimension peak capacity and peak capacity production rates, and how the sample type influences optimum second dimension gradient and re-equilibration times.

Keywords

2DLC; LC × LC; 2D On-line comprehensive chromatography; multidimensional separations; optimization; peak capacity; under-sampling; re-equilibration; cycle times; sampling times; peptides; gradient elution; isocratic elution

[*]To whom correspondence should be addressed (potts@gustavus.edu).

1. Introduction

High-resolution analytical techniques are essential when dealing with complex samples [1,2]. No single technique has the ability to fully characterize samples as complex as those encountered in proteomic [3] and metabolomic research [4]; however, comprehensive two dimensional liquid chromatography (2DLC) is attracting increasing attention due to its potential for very high resolving power in relatively short times compared to 1DLC. In principle 2DLC can greatly increase the peak capacity of HPLC over highly optimized one-dimensional HPLC. This improvement results mainly from the multiplicative relationship between the peak capacities of the first and second dimension separations and the total 2DLC peak capacity which leads to the so-called "peak capacity product rule" discussed by Karger, Snyder and Horvath [5], and later elaborated by Guiochon, et.al. [6] and Giddings [7]. Thus under *ideal conditions*, the total peak capacity of two-dimensional liquid chromatography ($n_{c,2D}$) is the product of the peak capacities of the first (^1n_c) and the second dimensions (^2n_c).

$$n_{c,2D} = {}^1n_c \times {}^2n_c \tag{1}$$

However, the 2DLC peak capacity given by Eq. 1 cannot be fully realized whenever the first dimension separation is "under-sampled" as is the case in nearly all experimental work [2]. To understand under-sampling effects it is perhaps best to think of a two dimensional chromatographic separation as a three step process. The first step is the first dimension separation, the second is the very critical step of "sampling" of the first dimension separation, and the third is the second dimension separation of the sample of first dimension effluent collected and transferred to the second dimension during the sampling step [2]. In multi-dimensional gas chromatography the sampling step is frequently termed the "modulation" step and the device which helps transfer the sample of the first dimension effluent to the second dimension column is called a modulator. This modulation or sampling step has been discussed extensively by Blumberg, and his work shows that it can be responsible for a considerable loss of the peak capacity predicted by Eq. 1 [8–10]. Clearly the consequences of the sampling step on the 2D peak capacity ($n_{c,2D}$) are not reflected in Eq. 1. Each of these three operations has an impact on the corrected 2DLC peak capacity, and in computing realistic estimates of the 2DLC peak capacity we need to correct for the loss in peak capacity due to the sampling step.

Choosing the proper sampling time is very important in practical 2DLC work. Murphy, Schure, and Foley (M-S-F) [11] developed a quantitative approach to estimating an under-sampling correction factor which has become the basis for a widely accepted sampling criterion [12–14]; it states that the effluent *must be sampled at least three or four times over the 8σ base width of a first dimension peak to avoid serious loss of resolution between a pair of peaks when the first dimension separation contributes heavily to the resolution*. The work of Murphy et al. was extended by Seeley [14], whose results for the 100% duty cycle case fully corroborate the findings of Murphy et al. Horie et al.[13] also investigated the under-sampling problem and concluded that *the optimum sampling time could be somewhat slower i.e. around 2 to 3.5 times across the 8σ basewidth of the first dimension peaks to realize the 2D peak capacity given by* Eq. 1. Blumberg and his coworkers [8,9] investigated the same problem in the context of gas chromatography and came to a similar conclusion. It is important to understand that all of this work [8–14] is based on the impact of under-sampling and reconstruction of the first dimension peak. The under-sampling and subsequent reconstruction of a single first dimension peak effectively broadens the peak, as perhaps most clearly explicated in the work of Blumberg [10].

Recently Davis et al.[12] significantly refined the seminal work of Murphy by taking a very different approach to estimating the effect of under-sampling and reconstruction. In essence their results are based on the simulation of entire 2D separations of multi-constituent samples, and include the effect of Poisson random retention time coordinates, exponentially random peak heights, and the effect of under-sampling on the number of observed peaks. Thus their results are based on the effect of under-sampling on the *entire* chromatogram and not just a single peak as was done in the work by Murphy. Interestingly their quantitative results differ only slightly from those of Murphy in the region of fast sampling (more than four samples per 8σ) but significant differences are seen in the severely under-sampled region. Because it is the first dimension that is under-sampled, an under-sampling correction factor is applied when calculating the first dimension peak capacity. Since the decision about sampling rate also affects the peak capacity in the second dimension, the two dimensions are related in complex ways.

The equation of Davis and coworkers is best written for present purposes as:

$$ {}^1n'_c = \frac{{}^1n_c}{\beta} = \frac{{}^1n_c}{\sqrt{1+\alpha * ({t_s}/{}^1w)^2}} \qquad (2) $$

Here ${}^1n_c$ represents the uncorrected first dimension peak capacity and ${}^1n'_c$ is the *corrected* peak capacity of the first dimension at the actual sampling rate and should be used in Eq. 1 when one is interested in a practically useful measure of 2D peak capacity. In the form used in Eq. 2 the *under-sampling coefficient*, α, was found to be 3.35 by Davis et al. for the situation in which the retention times are taken from a random population and all peaks heights being drawn randomly from an exponential distribution. The *"under-sampling correction factor"* (β) is defined implicitly in Eq. 2. The terms t_s and ${}^1w$ are the sampling time and first dimension peak width, which is taken as $4*{}^1\sigma$ (here ${}^1\sigma$ is the standard deviation of the first dimension peaks before sampling) such that the resolution of adjacent peaks will be unity. It is very important to recognize that the under-sampling correction depends upon the desired resolution. If a higher resolution were required then, everything else being held constant, one would have to sample faster. Thus we believe that α might well depend on the minimum resolution needed to separate two constituents and thus "see" two peaks. It is interesting to note that the method of Murphy et al. produces a value of α equal to about 1.83, indicating a smaller effect of under-sampling than found by us, while the approach taken by Blumberg using digital sampling theory yields a value of α equal to 4.00, which indicates a considerably larger effect of under-sampling. Finally, in unpublished work based on random retention distributions in two dimensions, Davis [15] showed that when the peak heights for the various components are assumed to be the same α is equal to 3.69. This work was also based on the assumption of random distributions of retention times. It is conceivable that the value of α will depend on additional considerations. For example, if multivariate detectors such as mass spectrometers and diode array absorbance detectors were used one might resolve peaks that are closer together [2,16] thus effectively mitigating some of the loss due to under-sampling and possibly effectively decreasing α. Similarly, digital curve resolution techniques which assume a peak shape function might make it possible to resolve peaks that have resolution values less than 0.5 [17–25].

Eq. 2 is central to this work wherein the goal is to investigate the *corrected* 2DLC peak capacity of the entire system (defined in Eq. 7 below). It should be realized that there is a strong interaction between the sampling time and other system parameters, especially the first dimension gradient time (${}^1t_g$) and first dimension peak width (${}^1w$), and therefore with the first dimension peak capacity. In order to appreciate the interrelatedness of the first

dimension sampling time and the timescale of the second dimension, one must understand how an on-line two dimensional system works. In on-line 2DLC [2] samples of the first dimension effluent stream are sequentially collected in a sample loop. After the loop is filled, its contents are redirected to the second dimension column, while first dimension effluent is directed into a second collecting loop during the same time period. The first loop contents must be eluted from the second dimension column before the second loop finishes filling. Clearly when only a single second dimension column is used (with exceptions, see [26]) the first dimension sampling time (t_s) can be no faster than, and is at best equal to, the second dimension cycle time (^2t_c). The second dimension column must be run on a much faster timescale than the first dimension separation to avoid under-sampling. Furthermore, if the second dimension separation is based on gradient elution, some portion of the sampling cycle time must be dedicated to loading the sample, flushing the gradient mixers, and bringing the column to a state of *"reproducible equilibrium"* as defined by Schellinger and coworkers [27–29]. These operations, while essential to the on-line method, require time in addition to the actual separation time on the column, and so limit somewhat the productivity of the on-line method. We note that off-line 2DLC does not require the combination of these "maintenance" processes with the sampling time, and, according to the analysis by Guiochon and coworkers [30–33], promises a higher potential overall 2D peak capacity than the on-line method. The overall analysis time of an off-line method, however, must be considerably longer than an on-line method (with identical first-dimension separation characteristics) due to sample handling and storage, limiting the possible productivity gains of higher peak capacities. Guiochon and coworkers estimate a 2D peak production rate of 4000 peaks in a 5.2 hour experiment (770 peaks per hour). As we will show below, our on-line 2DLC method, while delivering a maximum of only about 1000 peaks with a 22 s gradient in the second dimension and a 3 s re-equilibration time, but does so in only a 50 minute run time (a production rate of 1200 peaks per hour).

In our earlier work first dimension flow rates of 0.1 mL/min were used along with second dimension flow rates of 2–3 mL/min to ensure a complete solvent gradient within the sample loop filling time. Flow rates of 2–3 mL/min generate high column pressures when small particles and narrow columns are used. In our work 2.1 mm × 30mm or 2.1 mm × 33mm columns packed with 2.7 μm particles were used. Hot eluents were used to lower viscosities and thus pressures were greatly reduced and diffusion enhanced [33–40].

Here we evaluate the influence of key variables on the quantitative impact of under-sampling in 2D separations[L2] and expand upon our previous discussion [41] of a simple yet accurate model for estimating the total 2DLC peak capacity. This model reveals some complex interactions between the experimental variables (that is, the first and second dimension gradient times and the first dimension peak capacity) and allows us to identify practical steps that can be taken to optimize 2DLC separations efficiently.

2. Theory

We assume that gradient elution is used in both dimensions, the practical reasons for this choice in LC having been made clear in prior work [2,38]. In Eq. 2 we take the first dimension sampling time (t_s) to be equal to the second dimension separation *cycle time* (^2t_c), which is the sum of the second dimension gradient time (^2t_g) and the system re-equilibration time ($^2t_{reeq}$)

$$t_s = {}^2t_c = {}^2t_g + {}^2t_{reeq} \tag{3}$$

The use of a solvent gradient in the second dimension requires the resetting of solvent composition and column re-equilibration time at the end of each gradient. The sample loading and gradient delay times are also included in ${}^2t_g$. The re-equilibration process and its effectiveness have been discussed in an earlier paper [29]. No separation occurs in the second dimension column during the re-equilibration time, and it is a sacrifice made to ensure that every second dimension run is made with the column reproducibly equilibrated with the correct initial solvent mixture. Despite being "lost" time, t_{reeq} has an effect on the maximum corrected peak capacity [30], which is also explored here.

According to Snyder, *et.al*.[42], the peak capacity of a gradient separation can be reasonably *estimated* by Eq. 4:

$$ {}^1n_c = 1 + \frac{{}^1t_g}{w} \cong \frac{{}^1t_g}{w} \tag{4} $$

where the time window for the separation is maximized by taking it as t_g. This equation is clearly approximate in that no peaks can be observed before the dead time of the column under typical conditions. Eq. 4 is also based on the assumption that all peaks have the same width; this is never anything but approximately correct.

As before [41] substitution of Eqs. 3 and 4 in our implicit equation for β gives the following:

$$ \beta = \sqrt{1 + \alpha \left[\frac{{}^2t_c \, {}^1n_c}{{}^1t_g} \right]^2} \tag{5} $$

A representative plot of $1/\beta$ vs. ${}^2t_c$ is shown in Fig. 1. Inspection of Eq. 5 shows that at very short second dimension cycle times the correction factor (β) approaches unity but at long second dimension cycle times it becomes quite large. It is convenient to note here that when sampling is very slow, that is, when the second term under the root is dominant, the sampling correction factor reaches the limiting form:

$$ \beta \approx \sqrt{\alpha} \cdot \frac{{}^2t_c \, {}^1n_c}{{}^1t_g} \tag{6} $$

We now combine Eqs. 1, 2 and 5, and an important result for the corrected 2D peak capacity (defined as $n'_{\text{c,2D}}$) is obtained:

$$ n'_{c,2D} = \frac{{}^1n_c \times {}^2n_c}{\sqrt{1 + \alpha \left(\frac{{}^2t_c \, {}^1n_c}{{}^1t_g} \right)^2}} \tag{7} $$

Eq. 7 first appeared in an earlier paper from our laboratory [41]. It appears in a modified form in Horvath, et al. [32]. In Fig. 2 Eq. 7 is used to generate a representative plot of $n'_{\text{c,2D}}$ vs. ${}^2t_{\text{g}}$. It clearly shows that as the second dimension gradient time is increased (and thus ${}^2t_{\text{c}}$ is increased) there is at first an increase and followed by a decrease in $n'_{\text{c,2D}}$. In order to compute such a plot, experimental data (see below) relating the second dimension peak capacity to the second dimension gradient time must be used. We will show this relationship shortly. We will refer to the second dimension cycle time at the maximum value of $n'_{\text{c,2D}}$ as ${}^2t_{\text{c,opt}}$, and the corresponding second dimension gradient time as ${}^2t_{\text{g,opt}}$. Eq. 7 clearly

shows that the dependence of the total 2DLC peak capacity on the first dimension peak capacity (^1n_c) becomes progressively weaker when under-sampling sets in at the longer values of the second dimension cycle time, and the denominator in Eq. 7 becomes substantially greater than unity. As the degree of under-sampling worsens, the dependence of $n'_{c,2D}$ on ^1n_c becomes less than the first power as it would be under ideal conditions (see Eq. 1). When we take the limit as under-sampling becomes very severe (and combine Eqs. 1, 2 and 6) we see that *the dependence of the corrected 2DLC peak capacity on the first dimension peak capacity divides out entirely* and we obtain:

$$n'_{c,2D} \cong \left(\frac{1}{\sqrt{\alpha}}\right)\frac{^1t_g\,^2n_c}{^2t_c} \tag{8}$$

We refer to Eq. 8 as the “approximate model” [41]. Its accuracy and implications are discussed below.

3. Experimental

3.1 Materials and Reagents

All solutes were of reagent grade or better and were used without further purification. Acetophenone, butyrophenone, valerophenone, hexanophenone and heptanophenone and Trifluoroacetic acid (TFA), 99%, were purchased from Aldrich (Milwaukee, WI, USA). Eleven peptides (Gly-Phe, Neurotensin fragment 1-8, Phe-Phe, LHRH, Angiotensin II, [Val^5]-Antiogensin I, Substance P, Renin substrate, Momany peptide, Insulin chain B oxidized and Melittin) and Bovine Serum Albumin (BSA) were obtained from Sigma (St. Louis, MO, USA). Acetonitrile was obtained from Burdick and Jackson (Muskegon, MI). HPLC grade water was obtained in-house from a Barnstead Nanopure deionizing system (Dubuque, IA). This water was boiled to remove carbon dioxide and cooled to room temperature before use. All pure solvents were filtered through a 0.45-μm nylon filtration apparatus (Lida Manufacturing Inc., Kenosha, WI) before use. All eluent mixtures were prepared gravimetrically.

3.2 Measurement of Second Dimension Peak Capacity

In the work reported here the peak capacities of the second dimension column were measured with a Halo C18 type phase (MacMod Analytical, Chadds Ford. PA, 2.7 μm particle size, 90 Å pore size, and 2.1 × 33 mm or 2.1 × 30 mm). For the phenone series of compounds, each second dimension separation in the 2DLC separations consisted of a reversed-phase gradient from 20% solvent B to various final percentages of the B solvent depending on the gradient time; for the eleven peptide compounds, each second dimension separation in the 2DLC separations consisted of reversed-phase gradient from 5% solvent B to various final percentage of B solvent depending on the gradient time. In both cases the A solvent was 0.1% trifluoroacetic acid in water and the B solvent was pure acetonitrile. A flow rate of 3.0 mL/min was used throughout the experiment. The column was held at 100 °C by use of the heater described in [29]. The final %B was varied as the second dimension gradient time was increased to maximize the retention time window. For the phenone series, the total gradient cycle times used were 12, 21, 42, 63, 105, 147 and 189 s; the corresponding final %B values were 66.5, 55, 45, 37, 30 26 and 23 %, respectively. For the eleven peptide compounds, the gradient cycle times used were 9, 12, 15, 21, 42, 63, 84, 105, 147 and 189s. In both separations, the re-equilibration time for the second dimension HPLC column was fixed at 3s. The 3-s re-equilibration time corresponds to roughly two column volumes of solvent; one column volume is required to flush strong (acetonitrile-rich) solvent out of the fluidic components of the pumping system and the system connecting tubing, and

the second column volume is required to actually re-equilibrate the HPLC column to the extent that the repeatability of retention time in the second dimension is satisfactory (0.0005 min standard deviation[29]). LabVIEW 6.0 software and a 6024E data acquisition board (National Instruments Inc., Austin, TX) were used to control the coordination of the first dimension system, the 10-port sampling valve, second dimension pumping system, and photodiode array detector using simple programs written in-house. The Agilent HPLC instrumentation has been described in detail in an earlier paper [38].

The isocratic plate count of the 2.1mm × 30 mm Halo C18 column was measured using heptanophenone as a solute in 50:50 acetonitrile: water at 35 °C and interstitial linear velocities between 0.14 and 3.15 cm/s. The maximum plate count of the column was 1480 at 0.62 cm/s. At a linear velocity of 3.15 cm/s, a rate commonly used in the second dimension, the plate count was 920 ($k' = 11.2$).

The peak capacities reported here for the second dimension column were computed as the so-called "sample peak capacity" (n^*_c) developed by Snyder et al. [42] and used by us previously [43]

$$n_c^* = \frac{t_{R,n} - t_{R,1}}{w_{avg.}} \tag{9}$$

Here $t_{R,n}$ and $t_{R,1}$ are the retention times of the first and last peaks eluted from the column and w_{avg} is the average peak width taken as $4(^1\sigma)$ corresponding to a resolution of unity. This is a rather conservative estimate compared to other ways of computing the peak capacity [44,45].

4. Results and Discussion

4.1 Experimental Peak Capacity Data

As described above, a homologous series of alkylphenones and a separate set of peptides were used for measuring the second dimension peak capacity as a function of the second dimension cycle time, using the method of Wang and coworkers [46], which optimizes the performance of the column assuming that its length is not varied as one increases the second dimension gradient time, uses a fixed but maximum flow rate, and varies the final mobile phase composition to place the last peak near the end of the gradient. We point out that in practice as gradient time is increased one can improve the peak capacity by also using a longer column and simultaneously decrease the flow rate [46,48]. It makes a significant difference to do so in the first dimension of 2DLC but is not as important in optimizing the second dimension because the column must be kept short to limit the second dimension cycle time. Fig. 3a shows the observed peak capacities and the peak capacity production rates (units of peak capacity per min of second dimension gradient time, re-equilibration time fixed at 3.0 s) for the phenones. The behavior of the peptides is shown in Fig. 3b. Inspection shows that the peak capacity measurements are reasonably well fit (solid line) by equations 10a and 10b, which were chosen because they fit the data; their mathematical form has no fundamental significance [30].

$$^2n_c = 44.05 \times (1 - \exp(-0.04 * {}^2t_g) \quad \text{(phenones)} \tag{10a}$$

$$^2n_c = 109.0 \times (1 - \exp(-0.02 * {}^2t_g) \quad \text{(peptides)} \tag{10b}$$

The peak capacity increases quite rapidly at first, but reaches a plateau after about 1 min, as it must because the column length is fixed. The peak capacity production rate reaches a maximum at a cycle time (i.e. ^2t_g + 3.0 s here) of 15 to 20 s. The peak capacity computed using Eq. 10a is used as the second dimension peak capacity for the calculation of the 2DLC peak capacities as a function of second dimension cycle time as shown in Fig. 2 and all subsequent figures. Obviously, different second dimension columns with different lengths, particle size, etc., and systems with different pressures and temperatures, as well as the different solutes illustrated, will show different relationships between peak capacity and cycle or gradient time.

4.2 Influence of Under-sampling on the Two-Dimensional Peak Capacity

The most important consequence of the under-sampling problem is that it leads to the serious decrease in the corrected first dimension peak capacity (defined in Eq. 2) which ultimately, through Eq. 8, generates the maximum in plots of $n'_{c,2D}$ vs. the second dimension cycle time as shown in Fig. 2. The maximum (at $^2t_{g,opt}$) results from, first, the rapid rise in ^2n_c with ^2t_g (see Fig. 3 and Eq. 10) that gradually reaches a plateau. The maximum is then followed by a decline induced by the decrease in the corrected first dimension peak capacity as ^2t_g (and therefore ^2t_c) increases and under-sampling becomes more severe. The approximate model equation (Eq. 8) emphasizes the importance of both the second dimension peak capacity (^2n_c) and the second dimension peak capacity production rate ($^2n_c/^2t_c$). It should be clear that when the first dimension is under-sampled, as is typical in current LC practice [47], one should work near the maximum in the plot of the second dimension productivity (see Fig. 3) to maximize the 2D peak capacity ($n_{c,2D}$).

An important consequence of under-sampling is the predicted very weak dependence of the corrected (2D) peak capacity on the first dimension peak capacity when the sampling time becomes excessive [41,32]. This effect becomes quite evident in Fig. 4 as ^1n_c is increased. Above some “critical” value of ^1n_c the corrected (2D) peak capacity, $n'_{c,2D}$, no longer depends at all strongly on ^1n_c and ultimately an asymptote is reached, *independent of* ^1n_c, and this asymptote is equal to that given by Eq. 8. It is clear that the longer is the first dimension gradient time the higher is the limiting corrected peak capacity at a given sampling time, that is, ^2t_c, and the higher is the first dimension peak capacity at which the limit is achieved.

This is an important[L3] result. It strongly suggests that “heroic” efforts to maximize the first dimension peak capacity by using very high pressures and very small particles are largely a waste of effort unless one also dramatically increases the first dimension gradient time [2,49,50] or significantly decreases ^2t_c. Similarly, use of sets of monolithic columns to achieve great first dimension column length may similarly be relatively ineffective unless the appropriate first dimension gradient time and second dimension cycle time are also appropriately adjusted [13,26,51]. It is clear from Fig. 4 that increasing the first dimension gradient time has a definite beneficial effect on the limiting corrected (2D) peak capacity as suggested by Eq. 8.

Taking α equal to 3.35, algebra shows that the corrected first dimension peak capacity needed to produce a corrected (2D) peak capacity of 90% of the limiting value defined by Eq. 8, that is, the asymptote shown in Fig. 4, is given by:

$$ {}^{1}n'_{c,0.9} \geq 1.13\frac{{}^{1}t_g}{{}^{2}t_c} \tag{11}$$

If we insert Eq. 11 in Eq. 5 we see that this value of ${}^{1}n_c'$ corresponds to a $\beta_{0.9}$ value of 2.29 at this critical point. When ${}^{1}n_c$ is given taken as that given by Eq. 11, the corrected 2D peak capacity will be equal to 0.9 times the value given by Eq. 8. Based on Fig. 4 and the inequality in Eq. 11, one will rarely require a first dimension peak capacity greater than 150. This result also clearly shows that an increase in first dimension gradient time and a decrease in the second dimension cycle time allow larger effective values of the first dimension peak capacity to be used and thus larger effective 2D peak capacities to be obtained (see Eq. 8).

Fig. 5 shows a series of plots of the corrected 2D peak capacity as a function of first dimension peak capacity, calculated at several second dimension gradient times, from 5 s to 50 s. Each line has an arrow on its rising portion showing the location of ${}^{1}n_{c,0.9}$. It is apparent (see Eq. 8) that the heights of the plateaus (the corrected 2D peak capacity) depend on the second dimension gradient time, ${}^{2}t_g$, which has a strong influence on under-sampling. In principle, the least under-sampling in the data set used in the figure should occur when ${}^{2}t_g$ is only 5 seconds. The curve for ${}^{2}t_g$ = 10 s shows the greatest corrected 2D peak capacity of all the curves. The curve for ${}^{2}t_g$ = 10 s is higher than that at ${}^{2}t_g$ = 5 s because ${}^{2}n_c$ is greater at ${}^{2}t_g$ = 10 s. The corrected 2D peak capacity falls off at still higher values of ${}^{2}t_c$, although ${}^{2}n_c$ continues to increase, because the under-sampling effect worsens. A second important feature of Fig. 5 is the steepness of the curves, which increases as the second dimension gradient time increases, and then remains at an optimal value at longer second dimension gradient times.

The dependencies of both $n'_{c,2D,0.9}$ and ${}^{1}n_{c,0.9}$ on the second dimension gradient time, ${}^{2}t_g$, are shown in Fig. 6. The optimal range for ${}^{2}t_g$ is 8 to 15 s. In accordance with Eq. 11, the value of ${}^{1}n_{c,0.9}$ falls continuously over the full range of ${}^{2}t_g$. This shows that as ${}^{2}t_g$ increases under-sampling becomes more and more severe and thus the first dimension peak capacity becomes less important in determining the corrected 2D peak capacity. As the second dimension becomes more important, the approximate equation (Eq. 8) becomes a better estimator of the 2D peak capacity. Table 1 gives values of $n_{c,2D,0.9}$ and ${}^{1}n_{c,0.9}$ that are shown in Fig. 5. Also included are the under-sampling factors, β (from Eq. 5), at these ${}^{1}n_{c,0.9}$ points. It is important to note that when ${}^{2}t_g$ increases from 10 s to 15 s, the decrease in $n'_{c,2D,0.9}$ is only 0.8%. Furthermore, when ${}^{2}t_g$ increases from 10s to 20 s, the decrease in $n'_{c,2D,0.9}$ is only 5%. This is despite the fact that the ${}^{1}n_{c,0.9}$ drops by 26% and by 41% over the same two ranges. Clearly, the second dimension is becoming the more important dimension in terms of determining the peak capacity over this entire range in second dimension gradient time. As far as optimization is concerned, it makes far more sense for an analyst to work on improving ${}^{2}n_c$ than ${}^{1}n_c$ in this range of first dimension gradient times. In accord with Guiochon's work [30], use of off-line 2DLC will produce higher values of $n'_{c,2D}$ because one can use longer second dimension cycle times and get to higher second dimension peak capacities without causing more under-sampling. However, this is done at the cost of longer overall analysis times as noted in the introduction (section *1*).

4.3 Influence of α on the Corrected (2D) Peak Capacity

As pointed out above α depends on the model used to determine the effect of under-sampling on the corrected first dimension peak capacity. We currently prefer the value 3.35[12]. Because this value may be refined in the future by introduction of different data analysis methods we thought it useful to examine the effect of different values of α on the

corrected (2D) peak capacity. Fig. 7(a,b) shows how α changes the corrected 2D peak capacity as a function of the second dimension gradient time. Notice that increasing α lowers $n'_{c,2D}$. There is a small shift in ${}^2t_{g,opt}$, as described below.

When calculations are done with the first dimension gradient time of 50 min, shown in Fig. 7(b), the corrected peak capacity increases as predicted by Eq. 7. What we did not anticipate is the trend to longer times in ${}^2t_{g,opt}$ as α decreases. Table 2 shows the behavior at both 25 and 50 minute first dimension gradient times. Smaller α, i.e. less under-sampling, allows for longer gradient and cycle times in the second dimension, and yields larger corrected (2D) peak capacities.

4.4 Influence of Re-equilibration Time on Peak Capacity

A potential major advantage of using isocratic elution over gradient elution in the second dimension is the fact that no time is needed in isocratic work to flush out gradient delay (dwell) volume, or for column re-equilibration after a change in eluent composition. Guiochon and his co-workers have implicitly incorporated the effect of re-equilibration in their work [30,31] as this term is one of the factors that determine the number of fractions that are taken of the first dimension. However, in this study we make the dependence quite explicit and deal with values of the re-equilibration time that are typical of actual practice. To investigate this putative advantage we have examined the effects of re-equilibration time by calculations in which $n'_{c,2D}$ was studied as a function of ${}^2t_g$ at re-equilibration times of 0, 3, 6, and 12 s. It was assumed that ${}^1t_g$ = 25 min and ${}^1n_c$=100, and the empirical equation for ${}^2n_c$ (Eq. 10) was used. ${}^2t_g$ was varied from 1 to 36 s. Results are shown in Fig. 8. A re-equilibration time of zero seconds is not an experimental option in gradient elution, but is included to show the limiting behavior. There is clearly a loss of corrected (2D) peak capacity as re-equilibration time is increased. When re-equilibration time is increased from 3 to 6 seconds, there is a loss of ca. 12% in $n'_{c,2D}$ and an increase in ${}^2t_{g,opt}$ of about 2 seconds. There is also an apparent flattening of the curves and a shift in ${}^2t_{g,opt}$ to longer times as $t_{re\text{-}eq}$ increases.

A comparison of the flatness of these curves can be made with data used in Fig. 8, and compiled in Table 3. Flatness is evaluated here by finding the range around the ${}^2t_{g,opt}$ at each $t_{re\text{-}eq}$ in which the value of $n'_{c,2D}$ is 95% or more of the limiting value, $n'_{c,2D,max}$. The table shows the lower 0.95 limit and the span (hi-low) in seconds. The largest span is 19 s, which occurs when the re-equilibration time is 12 s. This means that an analyst would suffer a loss of no more than 5% of $n'_{c,2D}$ by choosing a second dimension gradient time anywhere in the range of 14 to 33 seconds. This wide range of “just-about-optimal” behavior lends flexibility to experiment design and lowers somewhat the demands on hardware with little compromise in data acquisition. By similar reasoning, if an analyst can tolerate a loss of 12% in peak capacity, a 6 s re-equilibration time could offer a smaller hardware challenge than a 3 s re-equilibration time and might be an acceptable trade.

4.5 Influence of Second Dimension Peak Capacity Equation Fit

Calculations with Eq. 12 (below), which is a generalized form of Eqs. 10a and 10b, were performed with several combinations of coefficients to better understand the behavior of second dimension peak capacity over a wide range of second dimension gradient times. In all cases we assume that fixed second dimension column length and flow rates are used (see section *4.1* and pertinent comments). According to previous studies in this lab such conditions do not always produce the highest possible peak capacities. Indeed, previous work shows that as gradient time is increased the best peak capacities are obtained by using progressively longer columns at lower flow rates while working at the maximum possible pressure drop [48]. Our objective here is not optimization but to show the impact on the

corrected 2D peak capacity of varying the relationship between second dimension peak capacity on gradient time. Eq. 12 is a transcendental function with both a pre-exponential coefficient ("a") and an exponential coefficient term ("b").

$$^2n_c = a \times (1 - \exp(-b * {}^2t_g) \quad (12)$$

Fig. 9 shows a family of curves with pre-exponential coefficient a = 40 and 80 and exponential coefficients b = 0.020, 0.040, and 0.080 s^{-1}. A "b" value of about 0.04 is what we obtain for low molecular weight (MW 120–200) molecules on a Halo column (Fig. 3 and Eq. 10). Clearly, the "a" coefficient is the plateau, i.e. limiting, value for the second dimension peak capacity; at long gradient times, the exponential term becomes quite small, leaving only the pre-exponential term. The exponential coefficient "b" has a strong influence on the slope of the same plot at shorter gradient times. As expected, the smaller the exponential coefficient, the earlier the second dimension peak capacity becomes independent of second dimension gradient time.

Fig. 10 shows second dimension peak capacity production rate as a function of second dimension cycle time. The values of "a" and "b" lead to major changes in the peak capacity production rate, $^2n_c/^2t_c$, as a function of second dimension cycle time. Larger "a" coefficients lead to increased peak capacity production rates. The apparent increase in flatness of the $^2n_c/^2t_c$ function at smaller "a" coefficients is an illusion; the percentage changes in the slopes of $^2n_c/^2t_c$ vs. ^2t_c in all three cases are identical. The peaks in the curves occur at the same value of ^2t_c, 14 s. Since a re-equilibration time of 3s is assumed, the optimum gradient time is 11s.

Fig. 11 shows peak production rates for different exponential coefficients all calculated with the same pre-exponential coefficient, "a" = 40. The results show that the exponential term, "b" has a strong influence on the peak production rate, larger "b" terms leading to greater maximum values of $^2n_c/^2t_c$ at shorter gradient times. Clearly, large "b" coefficients produce high maximum peak capacity production rates (103 for b = 0.08 vs. 35 for b = 0.02). But they also shorten the optimal second dimension cycle time (8 s for b = 0.08 vs. 16 s for b = 0.02) and also narrow the 90% range around the maximum (range 4–15 s for b = 0.08 vs. range 7–36 s for b = 0.02).

Fig. 12 shows the effect of the "a" coefficient at constant "b" on the corrected (2D) peak capacities It should be apparent from the figure that a larger "a" coefficient favors higher maximum corrected (2D) peak capacities. Although it is hard to tell from the figure, the optimum second dimension gradient time does not change with "a" (it is 15 s in both cases). The curve with a = 80 is, however, sharper, meaning that the 0.90 range around the optimal ^2t_g value is narrower than it is in when a = 40 (for a = 80, 0.90 range is 7.5 to 27s, while for a = 40, the range is 7.5 to 39s). In general we conclude that larger "a" and smaller "b" will act to improve the corrected 2D peak capacity.

4.6 Isocratic Elution vs. Gradient Elution in the Second Dimension

It remains to be seen if there is a performance advantage in 2D peak capacity and or 2D peak capacity per unit time in using an isocratic elution rather than fast gradient elution for the second dimension. In the limit of very short, let us say less than 10 s second dimension cycle times where the re-equilibration time is a substantial fraction of the cycle time, it is conceivable that isocratic elution will produce a higher peak capacity than gradient elution. However, we are convinced that for cycle times of 20 s or greater with our current equipment gradient elution produces higher peak capacities in addition to its inherent

advantages in other regards mentioned above. In this discussion, we have assumed that both first and second dimension separations are done in the reverse-phase (RP) mode.

All other factors being equal, the supposed advantage of using an isocratic second dimension separation is a saving of the time lost in gradient operation to instrument flushing and column re-equilibration required by gradient elution (see calculations above). Unfortunately, all other factors are not equal, the chief being that gained by gradient focusing of the sample as it arrives from the sampling valve and the concomitant minimization of extra column broadening effects which come from everything that happens to the sample prior to entry into the second column.

There are a number of other serious issues which favor the use of gradient elution in the second dimension: First, towards the end of the first dimension gradient elution separation the effluent will almost certainly be stronger than the solvent in the isocratic second dimension, and not only will there be no sample “focusing” but there will be extreme injection solvent peak broadening effects [52]. Second, based on all of our experience we anticipate that sample volumes of about 20 μL will have to be injected onto the very low dead volume fused-core particle columns used as the fast second dimension. A 2.1 mm × 30 mm column will likely have a dead volume of only about 50 μL due to low total porosity. Third, the tubing used in the second dimension column heater to get the sample up to the high temperature needed to do the very fast second dimension separation will cause a great deal of broadening [35,36]. For all of these reasons we believe it is highly advantageous to continue to use gradient elution in the second dimension. Notwithstanding the above problems we are attempting a more detailed treatment and work is in progress.

5. Conclusions

In this work we have explicitly evaluated the impact of key variables and expanded upon our previous discussion of a simple yet accurate model for estimating the total 2DLC peak capacity, expressed as the corrected (2D) peak capacity. This work reveals some complex interactions between the experimental variables (that is, the first and second dimension gradient times and the first dimension peak capacity) and allows us to identify practical steps that can be taken to optimize 2DLC separations efficiently.

Initially, we examined the contribution of the first dimension to the corrected 2D peak capacity. It is clear that the longer is the first dimension gradient time the higher is the limiting corrected peak capacity for a given sampling time, that is, ${}^{2}t_{c}$, and the higher is the first dimension peak capacity at which that limit is achieved. Once this limit is reached, however, improvement in the corrected (2D) peak capacity is made *only* by increasing the peak capacity of the second dimension column. This result suggests that “heroic” efforts to maximize the first dimension peak capacity by using very high pressures, very long columns or very small particles are largely a waste of effort unless one also greatly increases the first dimension gradient time and simultaneously decreases the first dimension sampling time.

Under-sampling is a serious limiting factor in 2DLC analysis. Perhaps the most important consequence of under-sampling is the predicted very weak dependence of the corrected (2D) peak capacity on the first dimension peak capacity when the sampling time relative to the temporal width of the first dimension peaks becomes excessive. As the second dimension becomes more important at longer sampling times, the approximate equation (Eq. 8) developed in the text is a good measure of 2D peak capacity.

We explore the effect of α, the under-sampling factor, on the quantitative impact of under-sampling. The equation for under-sampling predicts that it becomes less important (and peak capacities increase) as α is decreased. As α influences the optimal sampling time, our

calculations also show an unanticipated shift to longer times in the optimal second dimension gradient and cycle time with decreasing α. Advances in data analysis methods may decrease α, enhance resolution, and also relax the requirement for short second dimension cycle times.

The use of gradient elution in the second dimension requires that there be time taken during the cycle time to flush and re-equilibrate the column before the next batch of eluents is passed from the sample loop. This "lost" time, t_{reeq}, has the effect of decreasing the maximum corrected (2D) peak capacity; the longer the re-equilibration, the lower is the corrected (2D) peak capacity. Our calculations show a shift in the time at which the maximum corrected (2D) peak capacity occurs to longer second dimension cycle times, and a lessening of the sensitivity of corrected (2D) peak capacity to the re-equilibration time.

The pair of coefficients "a" and "b" in the function (see Eq. 12) used to fit plots of second dimension peak capacity as a function of second dimension gradient time are characteristic of the type of sample being studied. The "a" coefficient strongly determines the maximum value for the second dimension peak capacity (long times), while "b" plays a larger role at short times. A doubling in "a" doubles the second dimension peak capacity, while increasing "b" lowers the second dimension gradient time at which the peak capacity becomes independent of second dimension peak capacity. This means that larger "b" values lead to shorter optimum second dimension gradient and cycle times. Larger "b" values also reduce the range in ^2t_g in which the second dimension gradient time is 90% of its optimal value. Larger "a" values, however, do not affect the optimal second dimension gradient time (about 15 s in our calculations), but, like increased "b", also reduce the range in ^2t_g in which the second dimension gradient time is 90% of its optimal value.

Acknowledgments

This work was supported by a grant from the National Institutes of Health (Grant GM54585), Fellowship from the U.S. Pharmacopeia for X.L., Fellowship from the American Chemical Society Division of Analytical Chemistry and Faculty Start-Up Award from the Camille and Henry Dreyfus Foundation to D.R.S., and gifts from MacMod Analytical and the Agilent Foundation.

Glossary

(As much as possible we use Schoenmakers' terminology [53])

α	Under-sampling coefficient
a	Pre-exponential coefficient in fitted Eq. for ^2n_c
β	Under-sampling correction factor
b	Exponential coefficient in fitted Eq. for ^2n_c
k'	Solute retention factor (isocratic)
^1n_c	First dimension peak capacity
^2n_c	Second dimension peak capacity
$^1n'_c$	Corrected first dimension peak capacity ($^1n_c/\beta$)
$^1n'_{c,0.9}$	Corrected first dimension peak capacity at 90% of the limiting value
$n'_{c,2D}$	Corrected (2D) peak capacity (corrected for under-sampling)
$n'_{c,\,2D,0.9}$	Corrected (2D) peak capacity at 90% of the limiting value (corrected for under-sampling)

$n'_{c,2D,max}$	Corrected (2D) peak capacity at the limiting value (corrected for under-sampling)
N_{col}	Number of parallel columns used in second dimension
${}^2t_c$	Second dimension cycle time (sampling time of first dimension)
${}^1t_g$	First dimension gradient time
${}^2t_g$	Second dimension gradient time
${}^2t_{g,opt}$	second dimension gradient time at which corrected (2D) peak capacity is a maximum
$t_{re\text{-}eq}$	Second dimension re-equilibration time; part of cycle time
t_s	First dimension sampling time
w_{avg}	Average peak width taken as $4*{}^1\sigma$ corresponding to a resolution of unity

References

1. Schure, MR.; Cohen, SA., editors. Multidimensional Liquid Chromatography: Theory, Instrumentation and Applications. Wiley & Sons; New York: 2008.
2. Stoll DR, Li X, Wang X, Porter SE, Rutan SC, Carr PW. J Chromatogr A. 2007; 1168:3. [PubMed: 17888443]
3. Issaq HJ, Chan KC, Janini GM, Conrads TP, Veenstra TD. J Chromatogr B. 2005; 817:35.
4. Dunn WB, Ellis DI. Trends Anal Chem. 2005; 24:285.
5. Karger, BL.; Snyder, LR.; Horvath, C. An Introduction to Separation Science. Wiley & Sons; New York: 1973.
6. Guiochon G, Gonnord MF, Zakaria M, Beaver LA, Siouffi AM. Chromatographia. 1983; 17:121.
7. Giddings JC. Anal Chem. 1984; 56:1258A–1260A. 1262A, 1264A.
8. Blumberg LM. J Chromatogr A. 2003; 985:29. [PubMed: 12580467]
9. Blumberg LM, David F, Klee M, Sandra P. J Chromatogr A. 2008; 1188:2. [PubMed: 18313681]
10. Blumberg LM. J Sep Sci. 2008; 31:3358. [PubMed: 18798219]
11. Murphy RE, Schure MR, Foley JP. Anal Chem. 1998; 70:1585.
12. Davis JM, Stoll DR, Carr PW. Anal Chem. 2007; 80:461. [PubMed: 18076145]
13. Horie K, Kimura H, Ikegami T, Iwatsuka A, Saad N, Fiehn O, Tanaka N. Anal Chem. 2007; 79:3764. [PubMed: 17437330]
14. Seeley JV. J Chromatogr A. 2002; 962:21. [PubMed: 12198965]
15. Davis, JM. Communication to P W Carr. 2009.
16. Porter SE, Stoll DR, Rutan SC, Carr PW, Cohen JD. Anal Chem. 2006; 78:5559. [PubMed: 16878896]
17. Frans SD, McConnell ML, Harris JM. Anal Chem. 1985; 57:1552.
18. Bahowick TJ, Synovec RE. Anal Chem. 1995; 67:631.
19. Sinha AE, Hope JL, Prazen BJ, Fraga CG, Nilsson EJ, Synovec RE. J Chromatogr A. 2004; 1056:145. [PubMed: 15595544]
20. Sinha AE, Fraga CG, Prazen BJ, Synovec RE. J Chromatogr A. 2004; 1027:269. [PubMed: 14971512]
21. Hoggard JC, Synovec RE. Anal Chem. 2007; 79:1611. [PubMed: 17297963]
22. Watson NE, Siegler WC, Hoggard JC, Synovec RE. Anal Chem. 2007; 79:8270. [PubMed: 17896828]
23. Skov T, Hoggard JC, Bro R, Synovec RE. J Chromatogr A. 2009; 1216:4029.
24. Schure MR. J Chromatogr A. 1991; 550:51.
25. Bezermer E, Rutan SC. Chemom Intell Lab Syst. 2002; 60:239.

26. Tanaka N, Kimura H, Tokuda D, Hosoya K, Ikegamic T, Ishizuka N, Minakuchi H, Kazuki N, Shintani Y, Furuno M, Cabrera K. Anal Chem. 2004; 76:1273. [PubMed: 14987081]
27. Schellinger AP, Stoll DR, Carr PW. J Chromatogr A. 2008; 1192:43.
28. Schellinger AP, Stoll DR, Carr PW. J Chromatogr A. 2008; 1192:54. [PubMed: 18374933]
29. Schellinger AP, Stoll DR, Carr PW. J Chromatogr A. 2005; 1064:143. [PubMed: 15739882]
30. Horvath K, Fairchild J, Guiochon G. J Chromatogr A. 2009; 1216:2511. [PubMed: 19217110]
31. Fairchild JN, Horvath K, Guiochon G. J Chromatogr A. 2009; 1216:6210. [PubMed: 19631325]
32. Horvath K, Fairchild JN, Guiochon G. Anal Chem. 2009; 81:3879. [PubMed: 19382753]
33. Carr PW, Wang X, Stoll DR. Anal Chem. 2009; 81:5342. [PubMed: 19505090]
34. Yan B, Zhao J, Brown JS, Blackwell J, Carr PW. Anal Chem. 2000; 72:1253. [PubMed: 10740867]
35. Thompson JD, Brown JS, Carr PW. Anal Chem. 2001; 73:3340. [PubMed: 11476234]
36. Thompson JD, Carr PW. Anal Chem. 2002; 74:4150. [PubMed: 12199587]
37. Antia FD, Horváth C. J Chromatogr A. 1988; 435:1.
38. Stoll DR, Wang X, Carr PW. Anal Chem. 2008; 80:268. [PubMed: 18052342]
39. McNeff CV, Yan B, Stoll DR, Henry RA. J Sep Sci. 2007; 30:1672. [PubMed: 17623448]
40. Stoll DR, Cohen JD, Carr PW. J Chromatogr A. 2006; 1122:123. [PubMed: 16720027]
41. Li X, Stoll DR, Carr PW. Anal Chem. 2008; 81:845. [PubMed: 19053226]
42. Dolan JW, Snyder LR, Djordjevic NM, Hill DW, Waeghe TJ. J Chromatogr A. 1999; 857:1. [PubMed: 10536823]
43. Wang X, Barber WE, Carr PW. J Chromatogr A. 2006; 1107:139. [PubMed: 16412451]
44. Neue UD. J Chromatogr A. 2005; 1079:153. [PubMed: 16038301]
45. Neue UD. J Chromatogr A. 2008; 1184:107. [PubMed: 18164021]
46. Wang X, Stoll DR, Schellinger AP, Carr PW. Anal Chem. 2006; 78:3406. [PubMed: 16689544]
47. Davis, JM. Multidimensional Liquid Chromatography: Theory, Instrumentation, and Applications. Schure, MR.; Cohen, SA., editors. Wiley & Sons; New York: 2008. p. 49
48. Wang X, Stoll DR, Carr PW, Schoenmakers PJ. J Chromatogr A. 2006; 1125:177. [PubMed: 16777118]
49. Issaq HJ, Chan KC, Janini GM, Conrads TP, Veenstra TD. J Chromatogr B. 2005; 817:35.
50. Sandra K, Moshir M, D'Hondt F, Tuytten R, Verleysen K, Kas K, François I, Sandra P. J Chromatogr B. 2009; 877:1019.
51. Ikegami T, Hara T, Kimura H, Kobayashi H, Hosoya K, Cabrera K, Tanaka N. J Chromatogr A. 2006; 1106(1–2):112. [PubMed: 16343520]
52. Snyder, LR.; Dolan, JW. High-Performance Gradient Elution: The Practical Application of the Linear-Solvent-Strength Model. Wiley & Sons; New York: 2007.
53. Schoenmakers P, Marriott P, Beens J. LCGC Europe. 2003; 16:335.

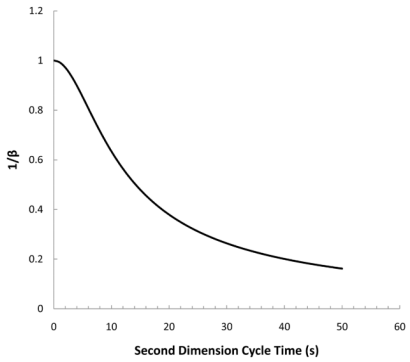

Fig. 1.

1/β as a function of second dimension cycle time. ${}^{1}t_{g}$ = 1500 s, ${}^{1}n_{c}$ = 100 peaks, α =3.35.

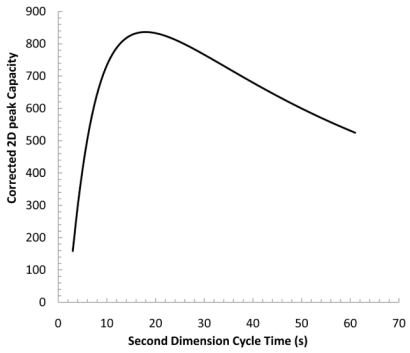

Fig. 2.

Corrected (2D) peak capacity as a function of second dimension cycle time. Note the maximum in $n'_{c,2D}$ at ${}^{2}t_{c,opt}$. The figure was generated using ${}^{1}t_{g}$ = 1500 s, ${}^{1}n_{c}$ = 100 peaks, α =3.35 and the relationship in Eq. 10a.

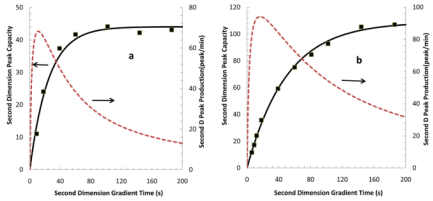

Fig. 3.

a,b. Peak capacity and peak capacity production vs second dimension gradient time for phenones and peptides. Eq. 10a,b plotted (left axes) and second dimension peak capacities per minute cycle time, assuming 3 second re-equilibration times, right axes. Data points shown were used to find the equations that are plotted with the solid lines. All data are for the 2.1 mm × 30 mm Halo column described in the experimental section using Eq. 9 as the basis for the peak capacity.

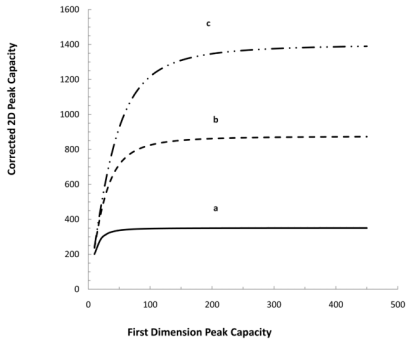

Fig. 4.

Plots of corrected (2D) peak capacity vs. first dimension peak capacity. ${}^{2}n_{c}$= 25 peaks, ${}^{2}t_{re\text{-}eq}$ = 3 s, ${}^{2}t_{c}$ = 20 s. Curve a: ${}^{1}t_{g}$ = 10 min, Curve b: ${}^{1}t_{g}$ = 25 min, Curve c: ${}^{1}t_{g}$ = 40 min.

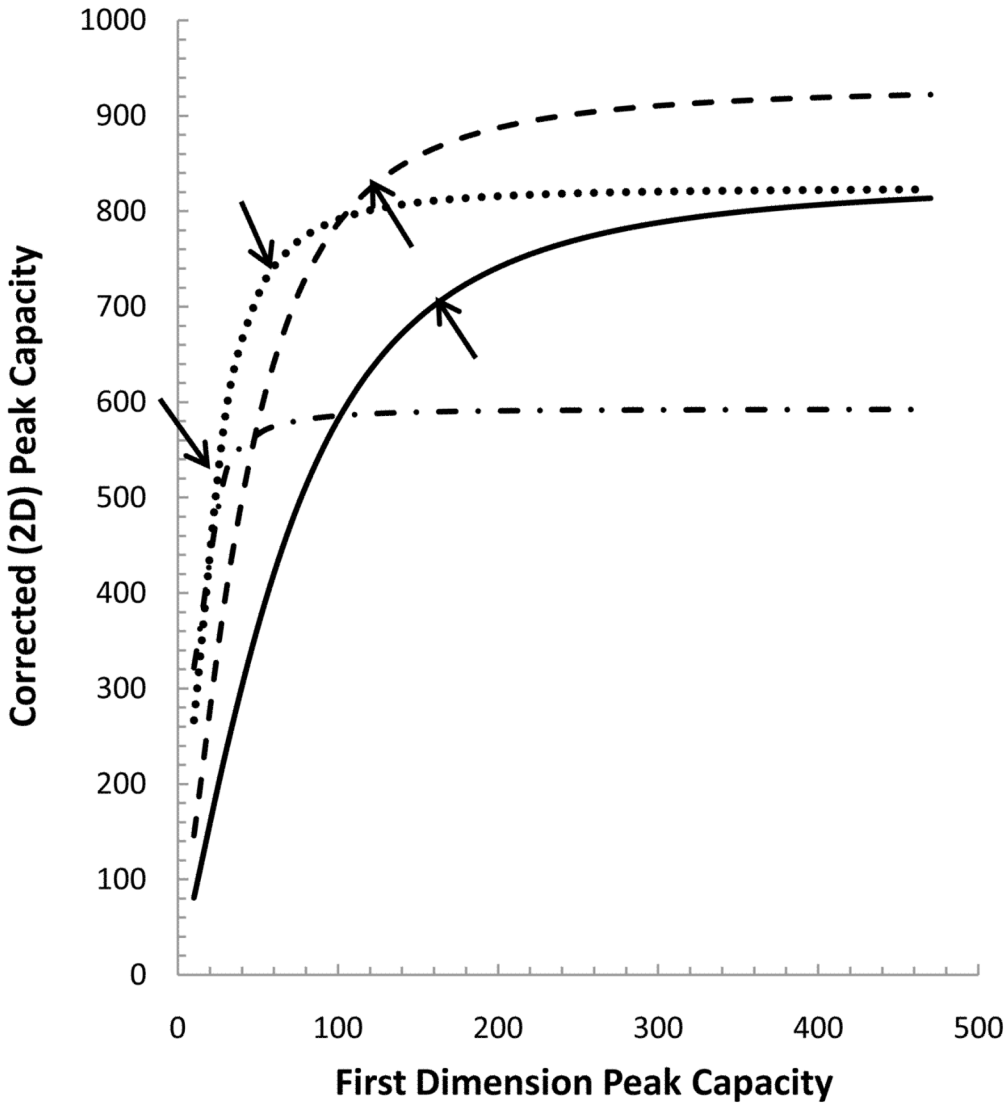

Fig. 5.

Effect of second dimension gradient time on corrected (2D) peak capacities as a function of first dimension peak capacities. Arrows point to the 90% peak capacities, beyond which only a 10% improvement in peak capacity can be expected. First dimension gradient time is 25 min. Second dimension re-equilibration time is 3 s. Second dimension peak capacities are calculated from Eq. 10. $^{2}t_{g}$ values: Solid line = 5 s, dash = 10 s, dot = 25 s, and dash-dot = 50 s.

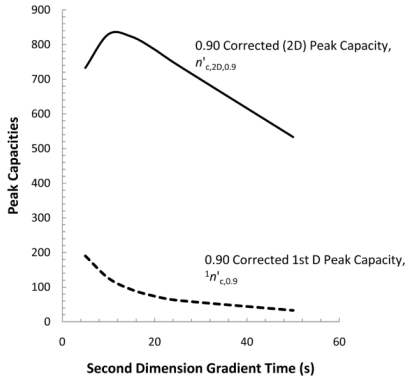

Fig. 6.

Corrected (2D) peak capacities ($n'_{c,2D}$ upper, solid) and corresponding corrected first dimension peak capacities ($^1n'_c$, lower, dashed) over a range in second dimension gradients times. First dimension gradient time is 25 min. Second dimension re-equilibration time is 3 s. Second dimension peak capacities are calculated from Eq. 10a.

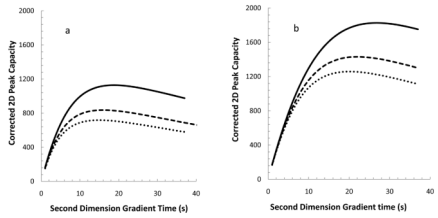

Fig. 7.

a and b. Corrected (2D) peak capacity vs. second dimension gradient time, showing the effects of α. First dimension peak capacity is 100 peaks and re-equilibration time is 3 s. ${}^{2}n_{c}$ calculated with Eq. 10a. First dimension gradient time is 25 min in (a) and 50 min in (b). Solid lines $\alpha = 1.60$, dash lines $\alpha = 3.35$, dot lines $\alpha = 4.80$.

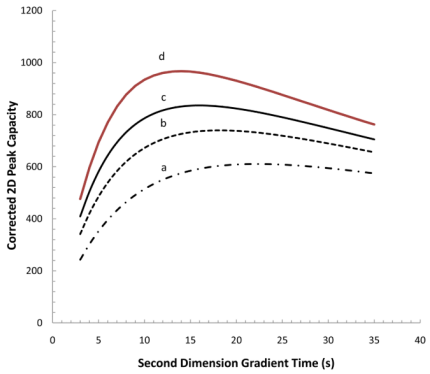

Fig. 8.

Corrected (2D) peak capacity as a function of second dimension gradient and re-equilibration time. First dimension gradient time is 25 min, first dimension peak capacity is 100. Eq. 10a used for ${}^{2}n_{c}$. ${}^{2}t_{reeq}$ values: d = 0 s, c = 3 s, b = 6 s, a = 12 s.

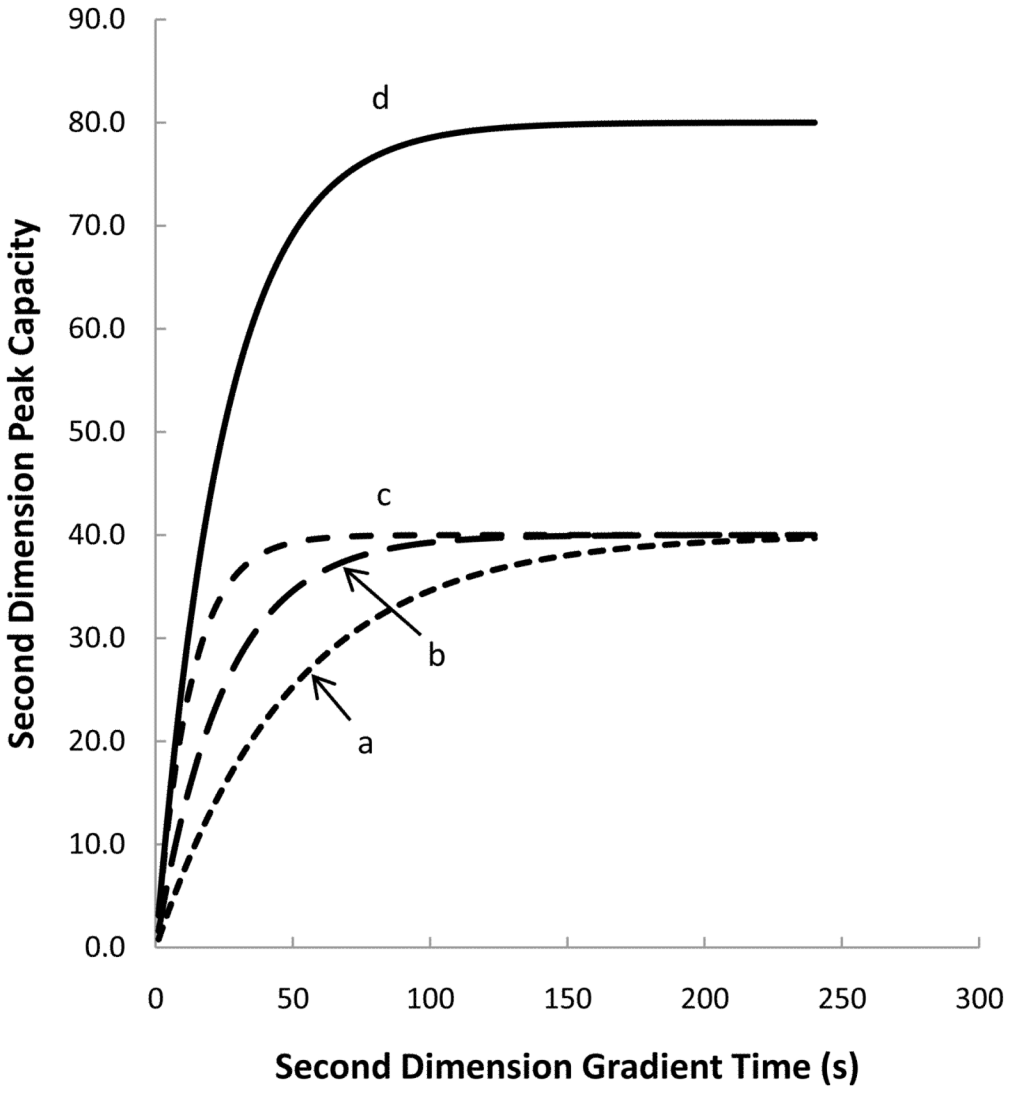

Fig. 9.

Plots of second dimension peak capacity vs. second dimension gradient time using Eq. 12 with different pre-exponential coefficients. Curve a: a = 40, b = 0.02; curve b: a = 40, b = 0.04; curve c: a = 40, b = 0.08; curve d: a = 80, b = 0.04.

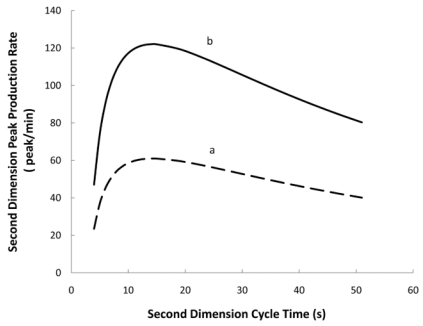

Fig. 10.

Second dimension peak production rate according to Eq. 12 for different coefficients. Curve a: a = 40, b = 0.04; curve b: a = 80, b = 0.04. Maxima occur at second dimension cycle time of 14 s in both cases.

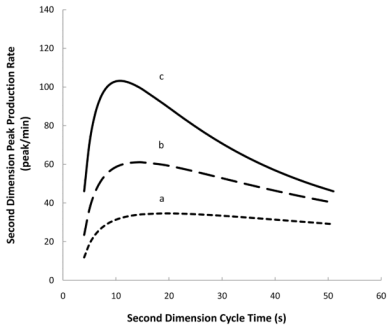

Fig. 11.

Second dimension peak production rate using different exponential coefficients in Eq. 12. All pre-exponential coefficients = 40, exponential coefficients for curve a: 0.02; curve b: 0.04; and curve c: 0.08.

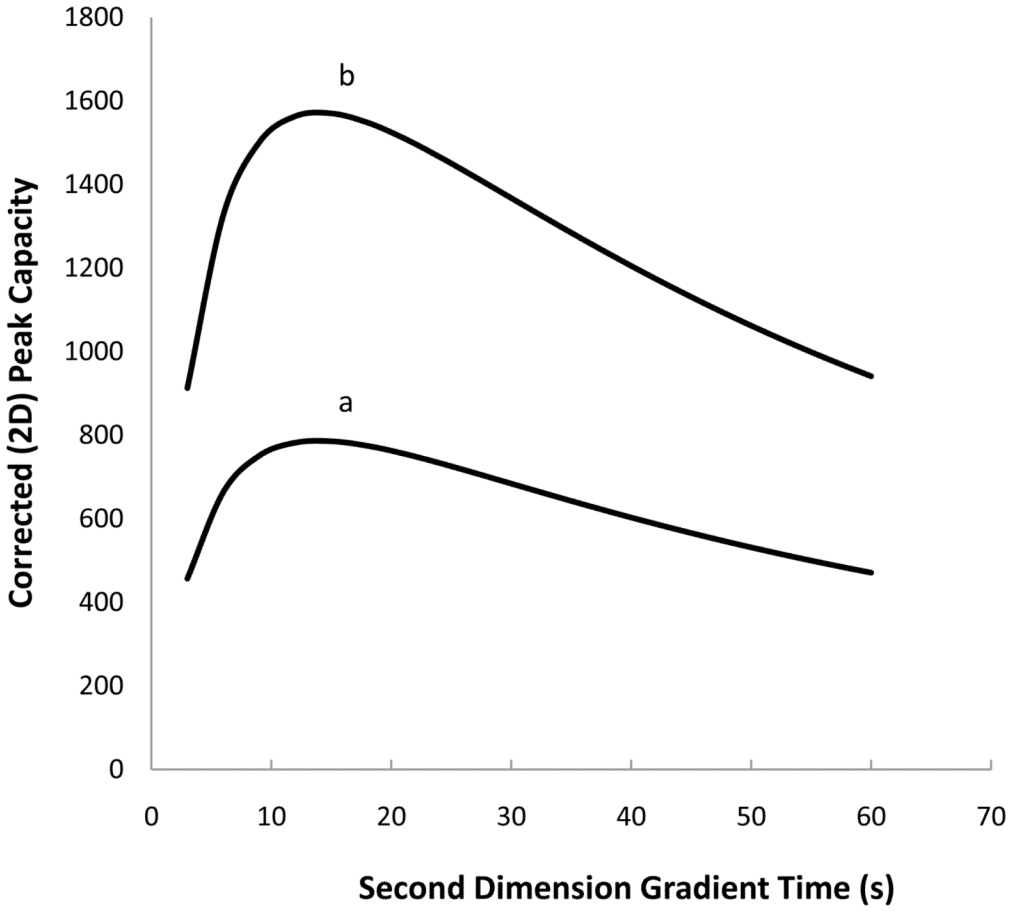

Fig. 12.

Corrected (2D) peak capacities over a range of second dimension gradient times. Plots for ${}^{1}t_{g}$ = 25 min, α = 3.35, ${}^{1}n_{c}$ = 150 peaks, ${}^{2}t_{re\text{-}eq}$ = 3s. Coefficients used in Eq. 12 to calculate ${}^{2}n_{c}$ in curve a: a = 40, b = 0.04; curve b: a = 80, b = 0.04.

Table 1

Critical $^{1}n_{c}$ values as a function of second dimension gradient times [a].

$^{2}t_{g}$(s)	$^{2}n_{c}$	$n'_{c,2D,0.9}$	$^{1}n_{c,0.9}$
5	8.1	733	190
10	14.8	830	126
15	20.2	823	93
20	24.6	786	74
25	28.2	741	62
50	38.3	533	33

Re-equilibration time is 3 s. $^{2}n_{C}$ values from Eq. 10, $n'_{C,2D}$ from Eq. 7 and maximum values at each $^{2}t_{g}$. β calculated from Eq. 5 with α = 3.35. $^{1}n_{C,\,0.9}$ values read from Fig. 5.

Table 2

Effect of α on corrected (2D) peak capacity and optimum second dimension gradient time[a]

	^1t_g = 25 min		^1t_g = 50 min	
α	$n'_{c,2D,max}$	$^2t_{g,opt}$(s)	$n'_{c,2D,max}$	$^2t_{g,opt}$(s)
1.60	1128	22	1825	30
3.35	836	16	1431	22
4.80	718	15	1258	20

[a]Data from Fig. 7a and b. $n'_{c,2D}$ calculated from Eq. 7, First dimension peak capacity is 100 and re-equilibration time is 3 sec. ^2n_c calculated with Eq. 10.

Table 3

Effect of re-equilibration time on the optimum second dimension gradient time, corrected (2D) peak capacity and upper and lower 95% points in Fig. 8.

$t_{re\text{-}eq}$(s)	$^2t_{g,opt}$(s)	$n'_{c,2D,max}$ [a]	fraction loss [c]	low ^2t_g(s) [b]	span(s) [b]
0	14	967	--	9.5	11.6
3	16	835	0.14	10.4	14.1
6	18	740	0.23	11.8	16
12	22	611	0.37	14.5	19.1

[a] $n'_{c,2D}$ is calculated with Eq. 7 using a set of ^2t_g values and specified $t_{re\text{-}eq}$. Maximum $n'_{c,2D}$ ($n'_{c,2D,max}$) are located by interpolation and corresponding ^2t_g values are found.

[b] The ranges of ^2t_g values over which $n'_{c,2D}$ is at least 95% of their maximum value are in the column labeled “span”. The lower ^2t_g values in the span are in the column “low ^2t_g(s)”

[c] Fraction loss is the loss of corrected (2D) peak capacity at each re-equilibration time relative to a hypothetical re-equilibration time of 0.0 s.